



## A STATISTICAL APPROACH TO COMPOSITE BEAMS

Krister Cederwall  
 Division of Structural Engineering, University  
 of Luleå, Professor and Head of the Department  
 of Civil Engineering

Kerstin Vännman  
 Department of Mathematics, University of Luleå,  
 Ph.D. and Senior Lecturer



Composite beams are analysed statistically with  
 level 2 methods. The effect of correlation between  
 different parameters is demonstrated.

Keywords: Composite beams, statistical analysis,  
 level 2 methods, correlated variables

### 1. INTRODUCTION

Composite beams demonstrate many features which make a probabilistic approach very desirable, e.g. a considerable variation within such material properties as strength and modulus of elasticity. Moreover, a strong correlation between stiffness and strength properties can exist. The effect on the failure risk of this correlation is of great interest.

In this paper the beam-action is treated for the special case of a rigid joint behaviour. The mechanical properties for this case are described (section 2). Simplified design methods presented by Cornell/2/ and Hasofer-Lind /9/ are used for the statistical analysis. These methods are briefly described (section 3). The described failure modes are treated from a statistical point of view with special regard to correlation between influential parameters (section 4). The difference in calculated formal failure risks for the different statistical methods used is demonstrated (section 4). In some special cases, we consider the complete beam structure when all the failure modes may occur (section 5).

## 2. MECHANICAL PROPERTIES

The overall view of the studied composite beam is to be seen in figure 2.1.

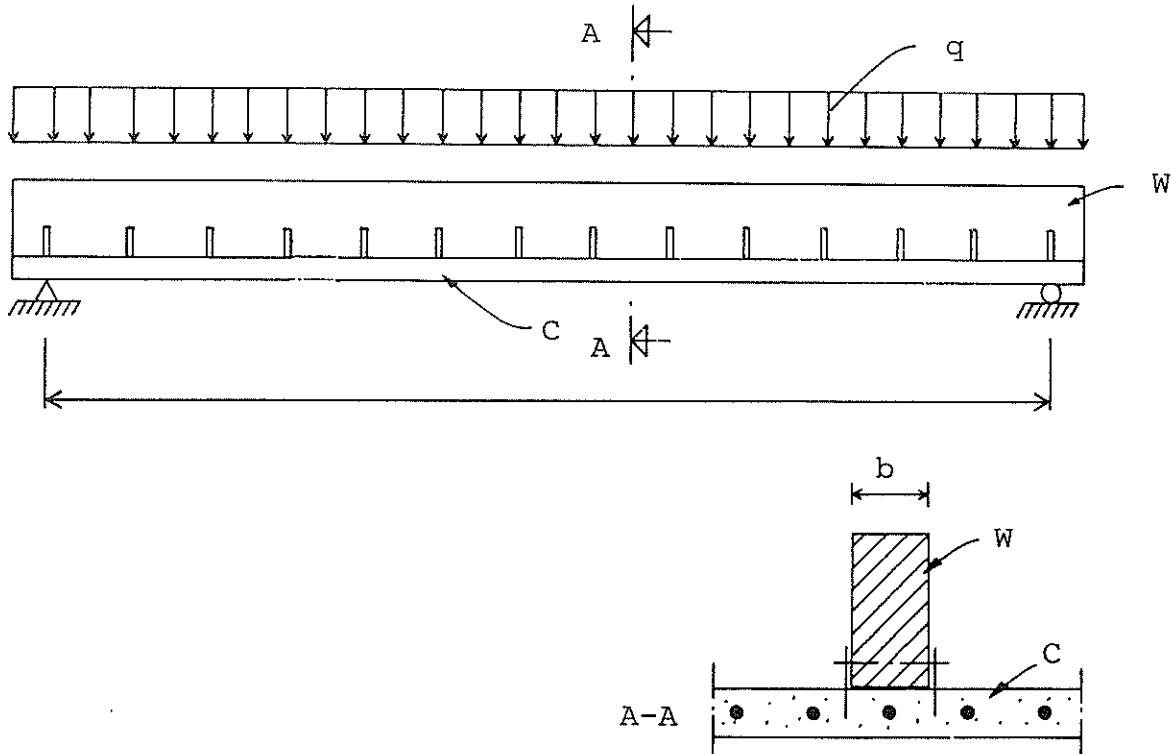


Fig 2.1 Overall view of composite beam

Wooden beams W are thus connected to a reinforced concrete slab C. The rigidity of the joint can be very stiff for instance by gluing or it can be flexible as for instance when the parts are joined by nailed steelplates.

In the following, we only treat the case with a rigid joint behaviour. We thus assume that there is no bond-slip between the different parts and failure of the joint is assumed to take place when the shear stress in the joint reaches the ultimate value  $f_j$ .

Bending failure can occur in a number of modes of which two are considered here, namely:

- a) Primary brittle failure in the wood-beam,
- b) Yielding of the reinforcement and secondary failure of the wood-beam.

The mechanical failure criteria of the bending modes are first

derived. For the analysis it is convenient to use the statical model according to figure 2.2.

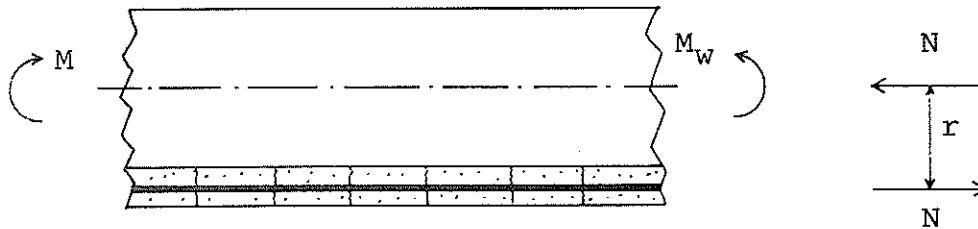


Fig 2.2 Statical model for the composite beam-action

The load-effect expressed as a bending moment  $M$  is thus giving rise to a bending moment  $M_w$  in the wooden beam and a couple  $N \cdot r$  where the compressive force  $N$  is resisted by the wooden beam and the tensile force  $N$  is resisted by the reinforcement of the concrete slab. The bending moment capacity of the concrete slab is neglected because of cracking. Already in the service limit state some cracking has occurred and the cracks propagate more or less through the whole depth of the slab. We have gained some experience from experimental tests /8/ which justify the assumptions made.

According to the assumptions made above the geometrical compatibility of the joint can be formulated as

$$(2.1) \quad \epsilon_s = \epsilon_w$$

where

$$\begin{aligned} \epsilon_s &= \text{strain in reinforcement} \\ \epsilon_w &= \text{strain in wooden beam} \end{aligned}$$

(transformed to the level of the steel reinforcement).

The material strains can be expressed as

$$(2.2) \quad \left\{ \begin{aligned} \epsilon_s &= \frac{N}{E_s A_s} , \\ \epsilon_w &= \frac{(M - N \cdot r) \cdot r}{E_w \cdot J_w} - \frac{N}{E_w A_w} , \end{aligned} \right.$$

where  $E_s$ ,  $E_w$  are the modulus of elasticity of steel and wood, respectively.  $A_s$ ,  $A_w$  are the areas of steel and wood, respectively, and  $J_w$  is the moment of inertia of the

wooden beam. From (2.1) and (2.2) we get

$$(2.3) \quad N = \frac{M}{r'}$$

where

$$(2.4) \quad r' = r + \frac{1}{r} \left( \frac{J_w}{A_w} + \frac{E_w}{E_s} \cdot \frac{J_w}{A_s} \right).$$

For a primary brittle failure in the wooden beam, the safety margin can be written as

$$(2.5) \quad Z = f_w - \sigma_w$$

where  $f_w$  is the bending strength of the wood and  $\sigma_w$  is the stress caused by the load on the beam. The safety margin is here defined in the following way:

$Z \leq 0$  corresponds to failure,

$Z > 0$  corresponds to the safe domain.

With

$$\sigma_w = \frac{M_w}{W_w} + \frac{N_{\max}}{A_w} = \frac{M - N_{\max} \cdot r}{W_w} + \frac{N_{\max}}{A_w}.$$

the equation (2.5) can be written as

$$(2.6) \quad Z = \frac{1}{W_w} \left\{ f_w \cdot W_w + N_{\max} \left( r - \frac{W_w}{A_w} \right) - M \right\}.$$

In (2.6)  $W_w$  is the symbol of the bending resistance of the wooden beam. With  $N_{\max}$  according to (2.3) the safety margin  $Z$  can be written in the following way

$$(2.7) \quad Z = \frac{r' - r + W_w/A_w}{r' W_w} \left\{ f_w \frac{r' W_w}{r' - r + W_w/A_w} - M \right\}.$$

For a primary yield of the reinforcement with a yield strength of  $f_s$ , the force  $N$  amounts to

$$(2.8) \quad N = f_s \cdot A_s$$

independent of the joint behaviour in the rest of the beam provided the joint capacity is large enough. In this case, the safety margin can easily be derived to be

$$(2.9) \quad Z = \frac{1}{W_w} \left\{ f_w \cdot W_w + f_s A_s \left( r - \frac{W_w}{A_w} \right) - M \right\}.$$

In order to compare different failure-modes it is more convenient to rewrite the expressions of the safety margins on a level corresponding to the beam load action  $q$ . Instead of eq. (2.7) and eq. (2.9) we thus get

$$(2.10) \quad Z = \frac{8f_w}{L^2} \frac{r' \cdot W_w}{r' - r + W_w/A_w} - q$$

and

$$(2.11) \quad Z = \frac{8f_w \cdot W_w}{L^2} + \frac{8f_s A_s}{L^2} \left( r - \frac{W_w}{A_w} \right) - q ,$$

respectively.

When analysing eq. (2.10) in a probabilistic manner it is interesting to study the effect of a strong correlation between  $E_w$  and  $f_w$  which is very often the case for real conditions. It is also possible that some correlation exists between  $E_w$  and  $q$  because of the fact that a stiffer beam will give a higher response for dynamic loads. When analysing eq. (2.11) it is from a theoretical point of view interesting to study correlation between the strength-values  $f_w$  and  $f_s$ . For most practical cases it is, however, to be expected that this correlation is nearly non-existent.

Joint failure will occur at the support for the treated loading case presented in fig. 2.1. The maximum support reaction  $R$  amounts to

$$R = \frac{qL}{2} = f_j \cdot b \cdot r'$$

corresponding to a safety margin

$$(2.12) \quad Z = \frac{2f_j \cdot b \cdot r'}{L} - q .$$

When analysing eq. (2.12) it is interesting to study the correlation between  $f_j$  and  $f_w$  which can be very strong. In this case we thus have a correlation between the different failure-modes according to (2.10), (2.11), and (2.12).

### 3. RELIABILITY INDICES

We will analyse the three described failure modes, whose safety margins are given by formulas (2.10), (2.11), and (2.12), using reliability indices according to both Hasofer-Lind /9/ and Cornell /2/. For a detailed description of these two methods see either /2/ and /9/ or a modern textbook, e.g. /7/. A description adjusted to suit the failure modes considered in this paper is found in /1/.

Consider the safety margin  $Z$  as a general function of  $n$  random variables  $Z_1, Z_2, \dots, Z_n$ , not necessarily independent, whose expectations, variances and covariances are known. Let  $\mu_i$  denote the expectation of  $Z_i$ ,  $i = 1, 2, \dots, n$ , and  $\sigma_{ij}$  the covariance between  $Z_i$  and  $Z_j$ ,  $i, j = 1, 2, \dots, n$ . Furthermore, let the safety margin be

$$(3.1) \quad Z = g(Z_1, Z_2, \dots, Z_n).$$

Then the corresponding limit state surface is given by  $g(z_1, z_2, \dots, z_n) = 0$  in the  $(z_1, z_2, \dots, z_n)$ -space on which the distribution of the random variable  $(Z_1, Z_2, \dots, Z_n)$  is defined. This limit state surface divides the  $\bar{z}$ -space into a failure region  $\{\bar{z}: g(z_1, z_2, \dots, z_n) \leq 0\}$  and a safe region  $\{\bar{z}: g(z_1, z_2, \dots, z_n) > 0\}$ .

Cornell [2] introduced a reliability index  $\beta$  defined as

$$(3.2) \quad \beta = \frac{\mu_Z}{\sigma_Z},$$

where  $\mu_Z$  denotes the expectation and  $\sigma_Z$  the standard deviation of  $Z$ . Geometrically,  $\beta$  can be described as the distance between  $\mu_Z$  and 0 measured in units of  $\sigma_Z$  (see figure 3.1).

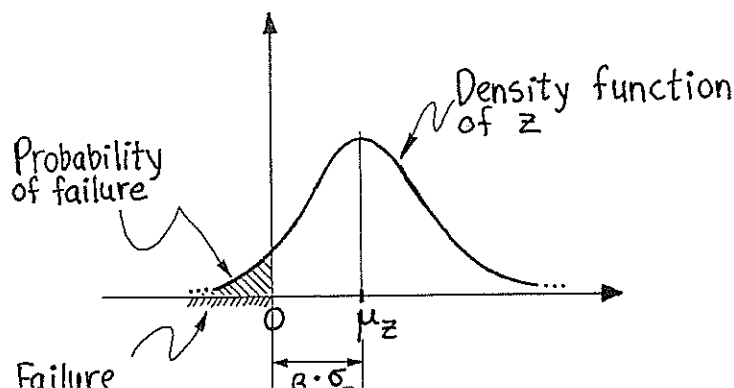


Fig 3.1

When  $g$  is a non-linear function of  $Z_1, Z_2, \dots, Z_n$  we cannot express  $\mu_Z$  and  $\sigma_Z$  exactly in  $\mu_i$  and  $\sigma_{ij}$ . The most straight-forward idea is then to approximate  $\mu_Z$  and  $\sigma_Z$  using a first order Taylor expansion of  $g$  around  $\mu_i, i = 1, 2, \dots, n$  (see e.g. /5/, /7/). Then we get the following approximation, usually called Cornell's index,

$$(3.3) \quad \beta_c = \frac{\mu_Z}{\sigma_Z} \approx \frac{g(\mu_1, \mu_2, \dots, \mu_n)}{\sqrt{\sum_{i=1}^n \sum_{j=1}^n \frac{\partial g}{\partial z_i} \frac{\partial g}{\partial z_j} \sigma_{ij}}}$$

To get Hasofer-Lind's index we first transform the variables  $Z_1, Z_2, \dots, Z_n$  into  $n$  uncorrelated and normalized variables  $X_1, X_2, \dots, X_n$ . (For details see e.g. /1/ or /7/.) Then the limit state surface  $g(z_1, z_2, \dots, z_n) = 0$  in the  $\bar{z}$ -space corresponds to a limit state surface  $h(x_1, x_2, \dots, x_n) = 0$  in the  $\bar{x}$ -space. The reliability index,  $\beta_{H-L}$ , according to Hasofer and Lind /9/, is now defined as the shortest distance, in the  $\bar{x}$ -space, between the origin and the limit state surface  $h(x_1, x_2, \dots, x_n) = 0$ . Hasofer-Lind's index can also be obtained from formula (3.2) if  $\mu_Z$  and  $\sigma_Z$  are approximated by using a first order Taylor expansion of  $g$  around the point on the limit state surface which is closest to the origin in the  $\bar{x}$ -space. When the limit state surface is a hyperplane Hasofer-Lind's reliability index  $\beta_{H-L}$  coincides with Cornell's index  $\beta_c$  in eq. (3.3).

As was first pointed out by Ditlevsen /4/, Cornell's index has a severe disadvantage. It is namely dependent on how the safety margin is defined. Hasofer-Lind's index does not have this problem of invariance of safety margins as was shown by Ditlevsen /4/.

#### 4. RESULTS

We first calculate Hasofer-Lind's index for the failure mode whose safety margin is defined in (2.10), i.e. for a primary brittle failure in the wooden beam. We consider the bending strength of the wood,  $f_w$ , the beam load action,  $q$ , and the modulus of elasticity of wood,  $E_w$ , as random variables. All the other parameters are assumed to be constant. Furthermore, we assume  $f_w$  and  $E_w$  to be positively correlated, while  $f_w$  and  $q$  as well as  $q$  and  $E_w$  are assumed to be uncorrelated. Set

$$(4.1) \quad Z_1 = f_w, \quad Z_2 = q, \quad Z_3 = E_w .$$

The limit state surface corresponding to the safety margin in (2.10) may now be written as

$$(4.2) \quad z_1 c_1 (c_2 + c_3 z_3) - z_2 (c_4 + c_3 z_3) = 0 ,$$

where

$$(4.3) \quad \begin{cases} c_1 = 8 W_w / L^2 , & c_2 = r^2 + I_w / A_w , \\ c_3 = I_w / (E_s A_s) , & c_4 = I_w / A_w + r W_w / A_w . \end{cases}$$

Let the expectation and variance of  $Z_i$  be  $\mu_i$  and  $\sigma_i^2$ , respectively,  $i = 1, 2, 3$ . Furthermore, let  $\rho_{13}$  denote the correlation coefficient between  $Z_1$  and  $Z_3$ . Using the covariance matrix  $(\sigma_{ij}) = (\rho_{ij} \sigma_i \sigma_j)$  of  $(Z_1, Z_2, Z_3)$ ' we can express the transformation leading to the uncorrelated and normalized random variables  $X_1, X_2, X_3$  explicitly. Hence the limit state surface in the  $\bar{x}$ -space

$$(4.4) \quad h(x_1, x_2, x_3) = 0$$

can be expressed explicitly. It can be shown that  $h$  can be written in the following form:

$$(4.5) \quad h(x_1, x_2, x_3) = a_{11} x_1^2 + a_{12} x_1 x_2 + a_{13} x_1 x_3 + a_{23} x_2 x_3 + a_{33} x_3^2 + b_1 x_1 + b_2 x_2 + b_3 x_3 + c_0 ,$$

where the coefficients  $a_{ij}, b_i, i, j = 1, 2, 3$  and  $c_0$  are functions of  $\mu_i, \sigma_i, i = 1, 2, 3, \rho_{13}, c_i, i = 1, 2, 3, 4$ . Their expressions require a considerable amount of space and are there-



fore left out. For details the reader is referred to /1/. To find Hasofer-Lind's index is now equivalent to finding the minimum distance between the origin and the surface  $h(x_1, x_2, x_3) = 0$ , the minimum distance being attained at the point P, say. Let  $(\alpha_1, \alpha_2, \alpha_3)'$  denote the unit vector from the origin towards P, see figure 4.1. Since, in our case,  $h$  is differentiable the Hasofer-Lind's index is the smallest  $\beta$  found by solving the system of non-linear equations

$$(4.6) \quad \begin{cases} h(\beta\alpha_1, \beta\alpha_2, \beta\alpha_3) = 0, \\ \alpha_i = -\frac{\partial h}{\partial x_i} / \sqrt{\sum_1^3 \left(\frac{\partial h}{\partial x_j}\right)^2}, \quad i = 1, 2, 3, \end{cases}$$

where the partial derivatives in (4.6) are evaluated at the point  $(\beta\alpha_1, \beta\alpha_2, \beta\alpha_3)$ . This method of solution is described e.g. in /7/.

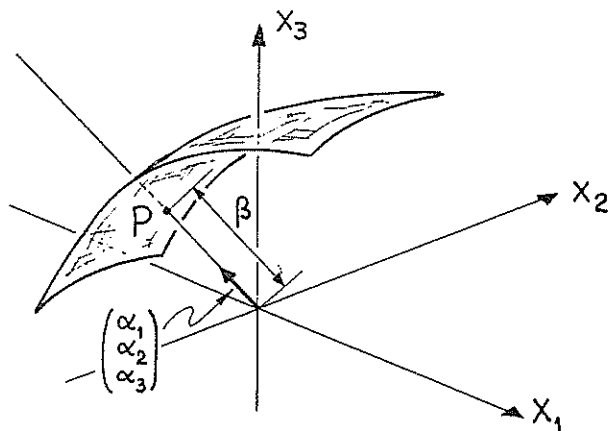


Fig 4.1

We have solved the system of equations in (4.5)-(4.6) using a standard routine from the NAG library called NAG C05NAF, see /10/.

The following realistic parameter values have been used:

$$\begin{aligned} b &= 0.05 \text{ m}, & h &= 0.15 \text{ m}, & r &= 0.1 \text{ m}, \\ A_s &= 2.0 \cdot 10^{-4} \text{ m}^2, & E_s &= 2.1 \cdot 10^5 \text{ MPa}, & L &= 4 \text{ m}. \end{aligned}$$

For the random variables the following expectations and standard deviations have been chosen (c.f. /8/). The material parameters  $\mu_1, \sigma_1, \mu_3, \sigma_3$  are a realistic choice considering a structural wood. The parameters  $\mu_2$  and  $\sigma_2$  for the load effect have been chosen to give reliability indices between 1.5 and 4.5.

<u>Random variable</u>	<u>Expectation</u>	<u>Standard deviatio.</u>
$Z_1 = f_w$	$\mu_1 = 40 \text{ MPa}$	$\sigma_1 = \mu_1/5$
$Z_2 = q$	$\mu_2 = 1 \cdot 10^{-3} (10^{-3}) 4 \cdot 10^{-3} \text{ MN/m}$	$\sigma_2 = \mu_2/3$
$Z_3 = E_w$	$\mu_3 = 1 \cdot 10^4 \text{ MPa}$	$\sigma_3 = \mu_3/5$

Hasofer-Lind's index has then been calculated according to the described method for  $\rho_{13} = 0.00 \text{ (0.05) } 1.00$ . In table 4.1 the results for  $\rho_{13} = 0.00 \text{ (0.10) } 1.00$  are stated. For more details see /1/. In table 4.1 we can see that the correlation between  $f_w$  and  $E_w$  does not change the reliability index  $\beta_{H-L}$  too much. But the index increases with  $\rho_{13}$ . According to /3/ a realistic value of  $\rho_{13}$  would be  $0.6 \leq \rho_{13} \leq 0.8$ .

As a comparison to Hasofer-Lind's index we have also calculated Cornell's index,  $\beta_C$ , according to eq. (3.3) with the limit state surface defined by (4.2). (For details see /1/.) The result is given in table 4.1 for the same parameter values as above.

Comparing Cornell's index  $\beta_C$  and Hasofer-Lind's index  $\beta_{H-L}$  in table 4.1, we find that they are almost the same when  $\rho_{13} = 0$  but

TABLE 4.1 Cornell's index,  $\beta_C$ , and Hasofer-Lind's index,  $\beta_{H-L}$ , for the limit state surface in eq. (4.2), corresponding to brittle bending failure, when the expected beam load,  $\mu_2$ , is varied

$\mu_2 \cdot 10^3$	1	2	3	4	1	2	3	4
$\rho_{13}$	$\beta_C$				$\beta_{H-L}$			
0.00	4.17	3.31	2.46	1.70	4.21	3.32	2.45	1.69
0.10	4.11	3.28	2.45	1.70	4.23	3.34	2.47	1.71
0.20	4.05	3.26	2.44	1.71	4.25	3.36	2.49	1.72
0.30	3.99	3.23	2.44	1.71	4.26	3.39	2.51	1.74
0.40	3.94	3.20	2.43	1.71	4.28	3.42	2.54	1.75
0.50	3.89	3.18	2.42	1.71	4.30	3.44	2.56	1.77
0.60	3.84	3.15	2.42	1.71	4.32	3.48	2.59	1.79
0.70	3.79	3.13	2.41	1.71	4.34	3.51	2.62	1.81
0.80	3.74	3.11	2.40	1.71	4.36	3.55	2.66	1.83
0.90	3.70	3.08	2.39	1.72	4.39	3.59	2.69	1.86
1.00	3.65	3.06	2.39	1.72	4.41	3.63	2.73	1.88

differ when  $\rho_{13}$  is larger. Furthermore, for  $\mu_2 \leq 3 \cdot 10^{-3}$  Cornell's index decreases with  $\rho_{13}$ , while Hasofer-Lind's index increases. It is easily shown (see /1/) that Cornell's index will decrease with  $\rho_{13}$  for  $\mu_2 < \mu_1 c_1$ , which is  $3.75 \cdot 10^{-3}$  in our case, and increase otherwise. The different behaviour in  $\rho_{13}$  depends on the fact that Cornell's index does not take account of the coefficients  $a_{ij}$  of the second-degree terms in the limit state surface in eq. (4.4)-(4.5), all of which depend on  $\rho_{13}$ . Hence, Cornell's index will give a misleading description of how the reliability depends on the correlation between  $f_w$  and  $E_w$ .

Since Cornell's index is not invariant we do not necessarily get the same behaviour of that index if we rewrite the limit state surface in (4.2). In /1/ Cornell's index has been calculated using another form of the limit state surface than the one in (4.2). The conclusions were the same as above, i.e. Cornell's index ought to be avoided when there are correlations present.

To visualize the situation described here we have made a picture of the limit state surface in (4.4)-(4.5) for  $\mu_2 = 2 \cdot 10^{-3}$  and  $\rho_{13} = 1$ . When  $\rho_{13} = 1$  we have two random variables only, and hence we can draw the limit state surface in the  $(x_1, x_2)$ -plane as a second degree curve (see figure 4.2).

In figure 4.2 the straight lines we get when approximating the limit state curve in accordance with Cornell's index and Hasofer-Lind's index, respectively, are also drawn. The two points denoted in figure 4.2 are those on the two lines closest to the origin. The minimum distances between the origin and each of the lines are  $\beta_C = 3.06$  and  $\beta_{H-L} = 3.63$ , respectively.

Corresponding pictures when  $\rho_{13} = 0$  and  $0.75$ , respectively, are given in /1/. We may conclude that when  $\rho_{13} = 0$  the two indices are almost the same,  $\beta_C = 3.31$  and  $\beta_{H-L} = 3.32$ , but the two approximating planes differ in orientation. When  $\rho_{13} = 0.75$ , which is a realistic value, the two planes are more alike in orientation but differ more in minimum distance,  $\beta_C = 3.12$  and  $\beta_{H-L} = 3.53$ . When  $\rho_{13} = 1$  the two lines are almost parallel but differ in minimum distance.

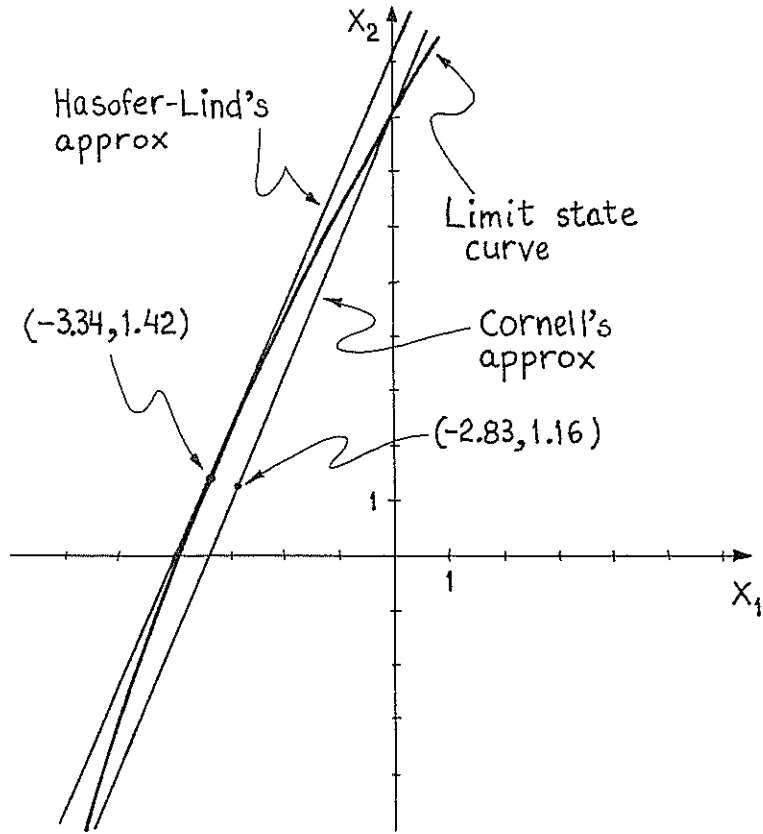


Fig 4.2 The limit state curve in (4.4)-(4.5), when  $\rho_{13} = 1$ , together with Cornell's and Hasofer-Lind's approximating lines

We will now study the failure mode whose safety margin is defined in (2.11), i.e. for a primary yield in the reinforcement and a secondary brittle failure in the wood. Here we consider the bending strength of the wood,  $f_w$ , the beam load action,  $q$ , and the yield strength of the reinforcement,  $f_s$ , as random variables, while all the other parameters are held constant. Furthermore, we assume  $f_w$  and  $f_s$  to be positively correlated, while  $f_w$  and  $q$  as well as  $q$  and  $f_s$  are assumed to be uncorrelated. Let, as before,  $Z_1 = f_w$ ,  $Z_2 = q$  and furthermore set

$$(4.7) \quad Z_4 = f_s .$$

The limit state surface corresponding to the safety margin in (2.11) may now be written as

$$(4.8) \quad c_1 z_1 + c_5 z_4 - z_2 = 0 ,$$

where

$$(4.9) \quad c_5 = 8A_s (r - W_w/A_w) / L^2$$

and  $c_1$  is defined in (4.3). Since the limit state surface (4.8) is a hyperplane Hasofer-Lind's index and Cornell's index coincide and may be written as

$$(4.10) \quad \beta_{H-L} = \beta_c = \frac{c_1 \mu_1 + c_5 \mu_4 - \mu_2}{\sqrt{c_1^2 \sigma_1^2 + \sigma_2^2 + c_5^2 \sigma_4^2 + 2c_1 c_5 \rho_{14} \sigma_1 \sigma_4}}$$

Here  $\mu_4$  and  $\sigma_4^2$  are the expectation and the variance, respectively, of  $Z_4$ , and  $\rho_{14}$  is the correlation coefficient between  $Z_1$  and  $Z_4$ . The index defined by eq. (4.10) has been calculated for the same parameter values as before with the addition of

$$\mu_4 = 500 \text{ MPa} \quad \text{and} \quad \sigma_4 = \mu_4 / 10 .$$

The result is given in table 4.2 for  $\rho_{14} = 0.00 \quad (0.10) \quad 1.00$ . We see that the index decreases with increasing correlation coefficient between  $f_w$  and  $f_s$ . Furthermore, the effect of the correlation coefficient on the index is worthwhile to observe for  $\mu_2 = 2 \cdot 10^{-3}$  and especially for  $\mu_2 = 1 \cdot 10^{-3}$ .

Eventually, we will calculate indices for the failure mode whose safety margin is defined in eq. (2.12), i.e. for a joint failure.

TABLE 4.2 Hasofer-Lind's index for the limit state surface in eq. (4.8), corresponding to plastic bending failure, when the expected beam load,  $\mu_2$ , is varied

$\mu_2 \cdot 10^3$		1	2	3	4
$\rho_{14}$	$\beta_{H-L}$				
0.00		7.20	5.13	3.45	2.22
0.10		6.97	5.01	3.39	2.20
0.20		6.75	4.90	3.34	2.17
0.30		6.56	4.79	3.29	2.15
0.40		6.38	4.69	3.24	2.13
0.50		6.21	4.60	3.19	2.11
0.60		6.06	4.51	3.15	2.08
0.70		5.91	4.43	3.11	2.06
0.80		5.78	4.35	3.07	2.04
0.90		5.66	4.28	3.03	2.03
1.00		5.54	4.21	2.99	2.01

The beam-load action,  $q$ , the modulus of elasticity of wood,  $E_w$ , and the strength of the joint,  $f_j$ , are considered as random variables. All the other parameters are assumed to be fixed. Here we assume  $E_w$  and  $f_j$  to be positively correlated, while all other pairs of random variables are uncorrelated. As before we let  $Z_2 = q$ ,  $Z_3 = E_w$  and furthermore set

$$(4.11) \quad Z_5 = f_j .$$

Let the expectation and variance of  $Z_5$  be denoted by  $\mu_5$  and  $\sigma_5^2$ , respectively, and let the correlation coefficient between  $Z_3$  and  $Z_5$  be denoted by  $\rho_{35}$ .

The safety margin in (2.12) gives raise to the same type of limit state surface as in eq. (4.2), but is less complicated, viz.

$$(4.12) \quad z_5 c_6 (c_2 + c_3 z_3) - z_2 = 0 ,$$

where

$$(4.13) \quad c_6 = 2b/(Lr)$$

and  $c_2$  and  $c_3$  are defined in (4.3). Hence we can utilize the calculations done earlier when determining the indices for eq. (4.12). In the transformed  $\bar{x}$ -space the limit state surface can be written in the same form as in (4.5). Then using the same method as earlier, we calculate Hasofer-Lind's index. The result, together with Cornell's index, is given in table 4.3 for  $\rho_{35} = 0.00$  (0.10) 1.00. The parameter values used are the same as earlier with the addition of

$$\mu_5 = 1.4 \text{ MPa} \quad \text{and} \quad \sigma_5 = \mu_5/10.$$

Here the value of  $\mu_5$  has been chosen to give an index around 3.5 when  $\mu_2 = 2 \cdot 10^{-3}$ .

In table 4.3 we see that both Cornell's index and Hasofer-Lind's index are decreasing with  $\rho_{35}$ . Furthermore, Cornell's index and Hasofer-Lind's index are almost the same when  $\mu_2 = 4 \cdot 10^{-3}$  and  $3 \cdot 10^{-3}$ . But when  $\mu_2 = 2 \cdot 10^{-3}$  and  $1 \cdot 10^{-3}$  they differ more. The correlation  $\rho_{35}$  between  $E_w$  and  $f_j$  does not change the index much when  $\mu_2 = 4 \cdot 10^{-3}$  and  $3 \cdot 10^{-3}$ . For smaller values of  $\mu_2$  the correla-

tion has a greater effect on the indices, however. It is here of great interest to observe that by changing the value of  $A_s$  from  $2 \cdot 10^{-4}$  to  $1 \cdot 10^{-4}$  the effect of the correlation on the indices becomes greater, especially for  $\mu_2 = 1 \cdot 10^{-3}$  and  $2 \cdot 10^{-3}$ . The results in this case, i.e. when  $A_s = 1 \cdot 10^{-4}$ ,  $\mu_2 = 1 \cdot 10^{-3}$  and  $\mu_2 = 2 \cdot 10^{-3}$  and all the other parameter values are as before, are stated in table 4.4.

TABLE 4.3 Cornell's index,  $\beta_C$ , and Hasofer-Lind's index,  $\beta_{H-L}$ , for the limit state surface in eq. (4.12), corresponding to brittle joint failure, when the expected beam load,  $\mu_2$ , is varied

$\mu_2 \cdot 10^3$	1	2	3	4	1	2	3	4
$\rho_{35}$	$\beta_C$				$\beta_{H-L}$			
0.00	6.45	3.76	2.01	0.91	6.80	3.82	2.02	0.91
0.10	6.28	3.70	1.99	0.91	6.70	3.77	2.00	0.91
0.20	6.12	3.65	1.98	0.90	6.61	3.72	1.99	0.90
0.30	5.97	3.59	1.96	0.90	6.52	3.68	1.97	0.90
0.40	5.84	3.54	1.94	0.89	6.43	3.64	1.95	0.89
0.50	5.71	3.49	1.92	0.89	6.35	3.60	1.94	0.89
0.60	5.59	3.45	1.91	0.88	6.26	3.56	1.93	0.88
0.70	5.48	3.40	1.89	0.88	6.18	3.52	1.91	0.88
0.80	5.37	3.36	1.88	0.87	6.10	3.49	1.90	0.88
0.90	5.27	3.31	1.86	0.87	6.03	3.45	1.88	0.87
1.00	5.17	3.27	1.85	0.86	5.95	3.42	1.87	0.87

TABLE 4.4 Cornell's index,  $\beta_C$ , and Hasofer-Lind's index  $\beta_{H-L}$ , for the limit state surface in eq. (4.12), corresponding to brittle joint failure, when the parameter  $A_s$  is changed to  $A_s = 1 \cdot 10^{-4}$

$\mu_2 = 10^3$	1	2	1	2
$\rho_{35}$	$\beta_C$		$\beta_{H-L}$	
0.00	6.34	4.32	7.31	4.55
0.10	6.10	4.20	7.15	4.45
0.20	5.88	4.09	6.99	4.36
0.30	5.68	3.99	6.83	4.28
0.40	5.51	3.90	6.68	4.20
0.50	5.35	3.81	6.54	4.13
0.60	5.20	3.73	6.40	4.06
0.70	5.06	3.66	6.27	3.99
0.80	4.94	3.59	6.15	3.93
0.90	4.82	3.52	6.04	3.87
1.00	4.71	3.46	5.93	3.81

We also see that Cornell's index and Hasofer-Lind's index in table 4.4 differ a lot for large values of the correlation coefficient. Hence, with correlation present Cornell's index is unreliable even for such an uncomplicated limit state surface as the one given by eq. (4.12).

Some overall-results of the analysis in this section are presented in figure 4.3, where the reliability indices,  $\beta_{H-L}$ , according to Hasofer-Lind are given for the different failure modes when the expected beam-load,  $\mu_2$ , is varied.

The plastic bending failure mode, when  $\rho_{14} = 0$ , will give the largest reliability index for the whole load domain. The brittle bending failure mode is relevant when the steel-yield strength is high and a complete deterioration of the wood takes place before the steel yields. In this latter case it is interesting to note that the failure mode depends upon the load domain. For  $\mu_2$  less

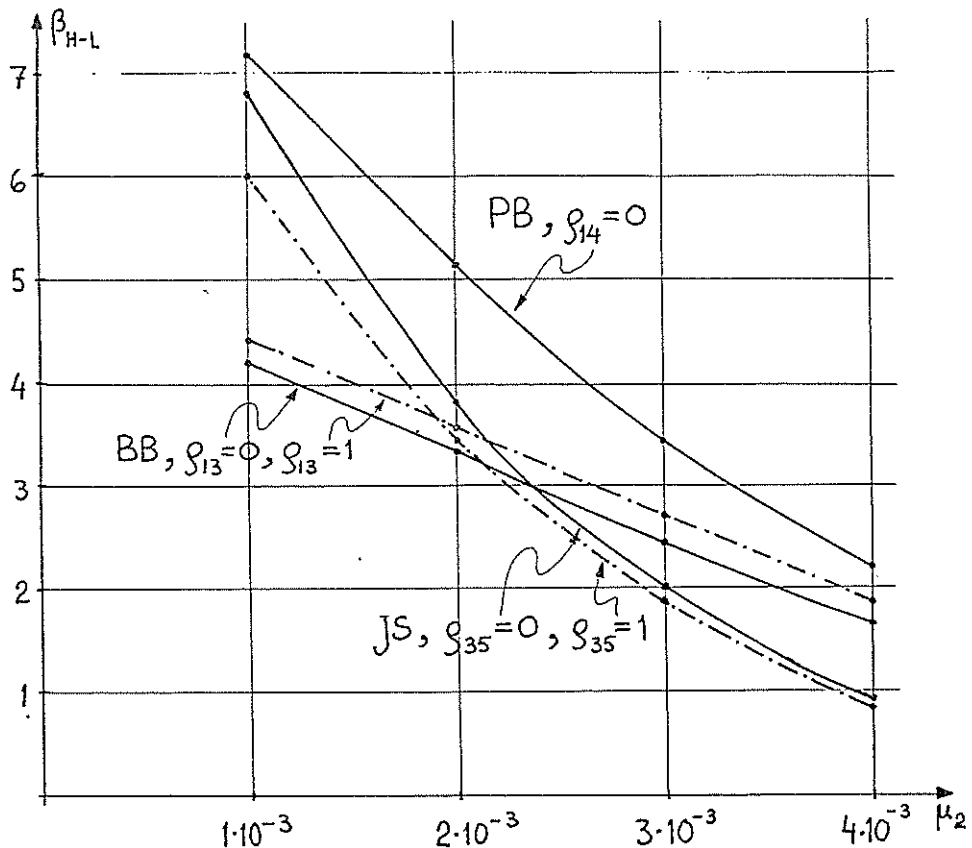


Fig 4.3 Hasofer-Lind's reliability index for different failure modes, when the expected beam load,  $\mu_2$ , is varied

- BB = Brittle bending mode (see table 4.1)
- PB = Plastic bending mode (see table 4.2)
- JS = Joint shear mode (see table 4.3)



than approximately  $2 \cdot 10^{-3}$  a brittle bending mode will give the smallest index and for  $\mu_2$  greater than  $2 \cdot 10^{-3}$  a joint-shear mode corresponds to the smallest index. Different correlations between strength and stiffness parameters may imply small changes in the boundaries of these different regions (see figure 4.3).

The overlapping effects of the different failure modes on the total risk of failure are commented upon in the next section.

## 5. FAILURE RISK FOR THE STRUCTURE

We will now, in some special cases, consider all the three failure modes described by eqs. (2.10), (2.11), and (2.12) together and take into account that the beam may fail in any one of the three modes. Hence the system will fail if at least one of the three safety margins in (2.10), (2.11), and (2.12) is negative.

Using the same notations as before, we have five random variables

$$(5.1) \quad Z_1 = f_w, \quad Z_2 = q, \quad Z_3 = E_w, \quad Z_4 = f_s, \quad \text{and} \quad Z_5 = f_j,$$

with the correlation coefficients  $\rho_{13}$ ,  $\rho_{14}$ , and  $\rho_{35}$  describing correlation between  $Z_1$  and  $Z_3$ ,  $Z_1$  and  $Z_4$ , and  $Z_3$  and  $Z_5$ , respectively. All the other pairwise correlations are assumed to be zero. To visualize the situation, we will first consider the case when

$$(5.2) \quad \rho_{13} = \rho_{14} = \rho_{35} = 1.$$

Then we may express the three mentioned safety margins in only two uncorrelated random variables, e.g.  $Z_1$  and  $Z_2$ . The three limit state curves in the  $\bar{x}$ -space  $h_i(x_1, x_2) = 0$ ,  $i = 1, 2, 3$ , corresponding to the safety margins in (2.10), (2.11), and (2.12), respectively, are second or first degree polynomials whose coefficients are easily expressed in  $\mu_i$ ,  $\sigma_i$ ,  $i = 1, 2, 3$ , and the constants  $c_i$ ,  $i = 1, 2, \dots, 6$ . (For details see /1/.) We illustrate these curves with  $\mu_2 = 2 \cdot 10^{-3}$ ,  $A_s = 2 \cdot 10^{-4}$  and the values of the remaining parameters as before. See figure 5.1.

The corresponding reliability indices according to Hasofer-Lind's index are in this case 3.63 for  $h_1$ , 4.21 for  $h_2$ , and 3.42 for  $h_3$  (see table 4.1, table 4.2, and table 4.3). To get the probability

of failure for the system we now have to integrate the probability density of  $(X_1, X_2)$  over the region where at least one failure will occur. Since we do not know enough of the behaviour of  $f_w$  and  $q$ , we assume, as a first approximation, that  $(X_1, X_2)$  has a standardized bivariate normal distribution. Instead of using a numerical integration method we may approximate the limit state curves by straight lines, since they are sufficiently flat in this case. We will approximate the limit state curves in accordance with Hasofer-Lind's index, i.e. with the tangent to the curve at the point closest to the origin, since then the probability for failure is approximately  $\Phi(-\beta_{H-L})$  for each failure mode. Using the mentioned approximation we get the approximating limit state lines as illustrated in figure 5.2. From figure 5.2 we see that the probability of failure for the system,  $P(F)$ , is

$$(5.3) \quad P(F) = P(F_1 \cup F_3) = P(F_1) + P(F_3) - P(F_1 \cap F_3) .$$

Using Hasofer-Lind's indices and bounds given by Ditlevsen in /6/ to estimate  $P(F_1 \cap F_3)$  we find (for details see /1/)

$$(5.4) \quad 0.000361 \leq P(F) \leq 0.000395 .$$

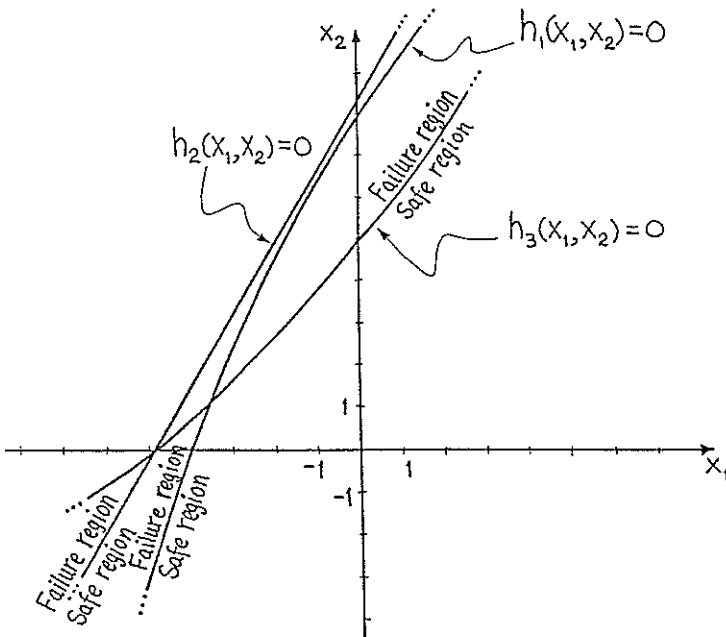


Fig 5.1 The limit state curves when  $\rho_{13} = \rho_{14} = \rho_{35} = 1$ .

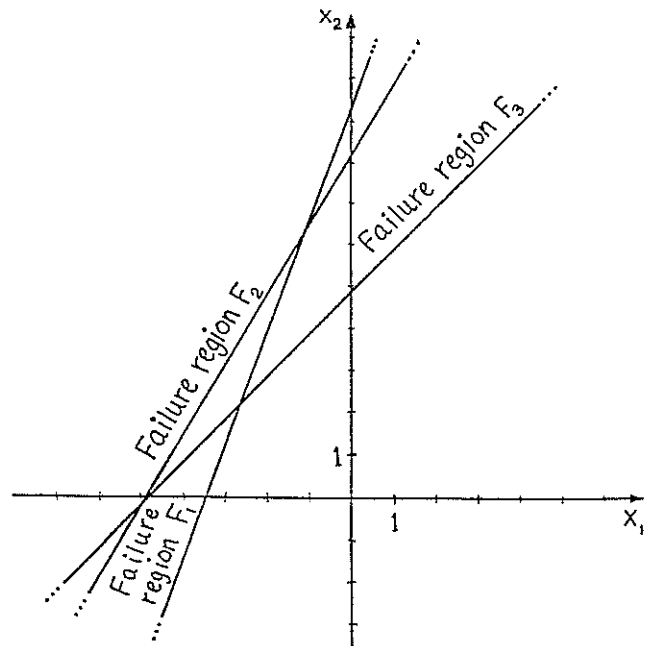


Fig 5.2 The approximate limit state curves when  $\rho_{13} = \rho_{14} = \rho_{35} = 1$ .

But here we must bear in mind that the limit state curves have been approximated by straight lines and we have assumed normality. The assumption of normality may be done formally, however, if we use Ditlevsen's generalized second moment reliability index, see /5/ or /7/. In that case we can define a generalized second moment reliability index for the system as

$$(5.5) \quad \beta_G = \Phi^{-1}(P(F)) .$$

According to (5.4) we can then give bounds for the index and get

$$(5.6) \quad 3.35 \leq \beta_G \leq 3.39 .$$

This generalized second moment index may be compared to the three mode reliability indices  $\beta_1 = 3.63$ ,  $\beta_2 = 4.21$ , and  $\beta_3 = 3.42$  according to Hasofer-Lind.

Still another special case, that is simple to visualize, is when

$$(5.7) \quad \rho_{13} = 1 , \quad \rho_{14} = 0 , \quad \rho_{35} = 1 .$$

The three limit state surfaces in this case are illustrated in figure 5.3. The corresponding reliability indices according to Hasofer-Lind are in this case  $\beta_1 = 3.63$ ,  $\beta_2 = 5.13$ , and  $\beta_3 = 3.42$ . This case is more realistic than the first case considered, since  $\rho_{14}$  in practice will be very close to 0. We will use the same idea as above and approximate the surfaces with hyperplanes according to Hasofer-Lind's index and assume that  $(X_1, X_2, X_4)$  has a standardized trivariate normal distribution. With  $F_1$ ,  $F_2$ , and  $F_3$  denoting the failure sets after approximation (see figure 5.4), we have the probability of failure,  $P(F)$ , given by

$$(5.8) \quad P(F) = P(F_1 \cup F_2 \cup F_3) .$$

To calculate  $P(F)$  we use bounds derived by Ditlevsen /6/. After tedious calculations we get

$$0.00035 \leq P(F) \leq 0.00039 ,$$

corresponding to the generalized index

$$3.35 \leq \beta_G \leq 3.39 .$$

Hence the reliability index for the system is about the same as

when  $\rho_{14} = 1$ . Using the method described it is possible to consider how the different failure modes influence the reliability for the system for other parameter values than the special ones studied here. It is also possible to use other approximation methods than the one described here. It is the intention of the authors to treat this subject more in detail in a future paper.

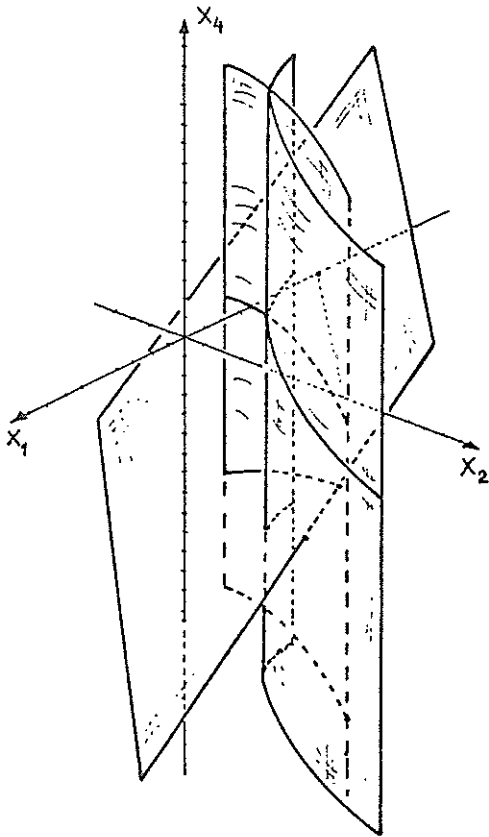


Fig 5.3 The limit state surfaces when  $\rho_{13} = \rho_{35} = 1, \rho_{14} = 0$ .

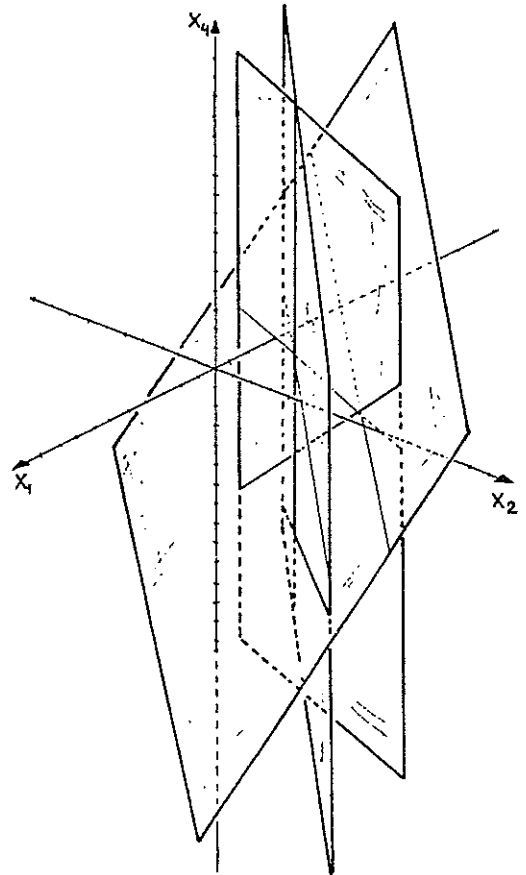


Fig 5.4 The approximate limit state surfaces when  $\rho_{13} = \rho_{35} = 1, \rho_{14} = 0$ .

REFERENCES

- /1/ CEDERWALL, K. and VÄNNMAN, K. (1982): Composite beams from a statistical point of view. Technical report 1982:05T, Division of Structural Engineering, University of Luleå
- /2/ CORNELL, C.A. (1969): A probability-based structural code. ACI Journal, Vol 66, pp 974-985
- /3/ CURRY, W.T. and FEWELL, A.R. (1977): The relations between the ultimate tension and ultimate compression strength of timber and its modulus of elasticity. Research report CP 22/77, Building Research Establishment, Princes Risborough Laboratory, Aylesburg, Buckinghamshire
- /4/ DITLEVSEN, O. (1973): Structural reliability and the invariance problem. Research Report No. 22, Solid Mechanics Division, University of Waterloo, Waterloo, Canada
- /5/ DITLEVSEN, O. (1979): Generalized second moment reliability index. J. Struct. Mech. Vol 7, No. 4, pp 435-451
- /6/ DITLEVSEN, O. (1979): Narrow reliability bounds for structural systems. J. Struct. Mech. Vol 7, No. 4, pp 453-472
- /7/ DYRBYE, C. et al (1979): Konstruktioners sikkerhed. Den private Ingeniørsfond ved Danmarks tekniske højskole, København
- /8/ GIRHAMMAR, U.A. (1979): Provning av RABO väggelement. (Tests of RABO wall-elements), Research report TULEA 1979:29, University of Luleå, Luleå
- /9/ HASOFER, A.M. and LIND, N.C. (1974): An exact and Invariant First-Order Reliability Format, Proc. ASCE, Journal of the Engineering Mechanics Division, Vol 100, pp 111-121
- /10/ NAG LIBRARY MANUAL, MARK 8 (1980). Numerical Algorithms Group, 7 Banbury Road, Oxford, U.K.